

Transpiration and Thermophoresis Effects on Non-Darcy Convective Flow Past a Rotating Cone with Thermal Radiation

B. Mallikarjuna, A. M. Rashad, Ahmed Kadhim Hussein & S. Hariprasad Raju

Arabian Journal for Science and Engineering

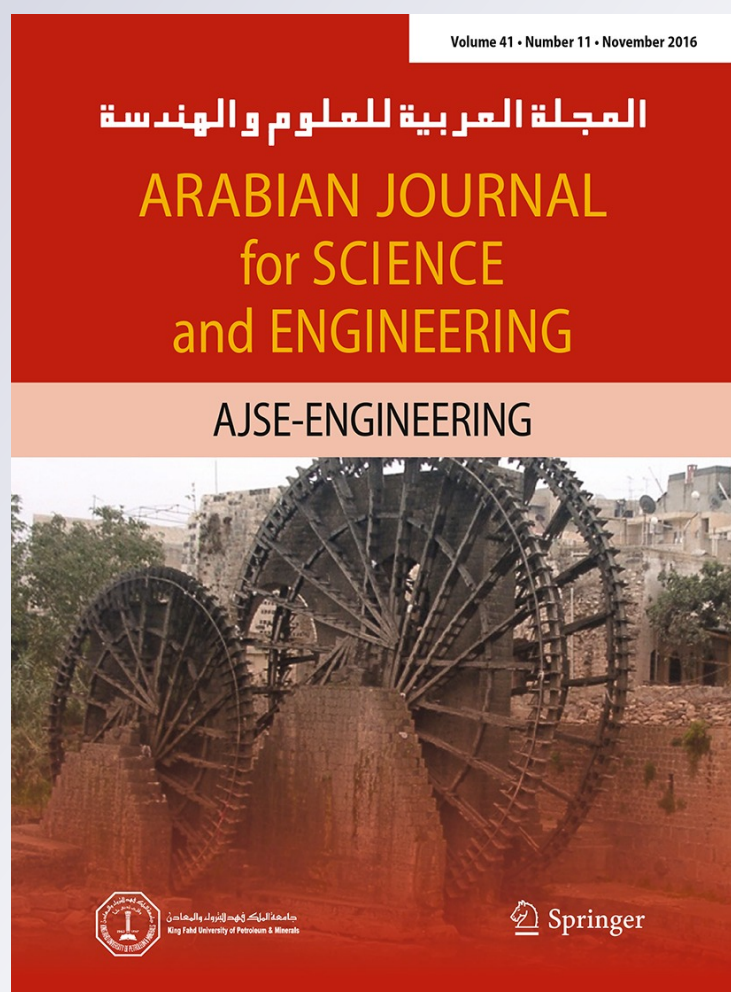
ISSN 1319-8025

Volume 41

Number 11

Arab J Sci Eng (2016) 41:4691-4700

DOI 10.1007/s13369-016-2252-x



Your article is protected by copyright and all rights are held exclusively by King Fahd University of Petroleum & Minerals. This e-offprint is for personal use only and shall not be self-archived in electronic repositories. If you wish to self-archive your article, please use the accepted manuscript version for posting on your own website. You may further deposit the accepted manuscript version in any repository, provided it is only made publicly available 12 months after official publication or later and provided acknowledgement is given to the original source of publication and a link is inserted to the published article on Springer's website. The link must be accompanied by the following text: "The final publication is available at link.springer.com".

Transpiration and Thermophoresis Effects on Non-Darcy Convective Flow Past a Rotating Cone with Thermal Radiation

B. Mallikarjuna¹ · A. M. Rashad² · Ahmed Kadhim Hussein³ · S. Hariprasad Raju⁴

Received: 21 September 2015 / Accepted: 13 June 2016 / Published online: 28 June 2016
© King Fahd University of Petroleum & Minerals 2016

Abstract In this article, mathematical model is developed for transport phenomena in an incompressible viscous fluid regime adjacent to a rotating vertical cone with thermal radiation and transpiration effects. The governing equations for the pertinent geometry are non-dimensionalized by employing specified transformations. A set of resultant equations are solved by numerical method. The solutions of this model are carried out under physical realistic boundary conditions to compute velocities, temperature and concentration functions distributions. The results are compared with previously available existing results. The excellent agreement has been found. The effect of thermal radiation, transpiration (surface injection/suction) and Forchheimer parameters, thermophoretic coefficient and relative temperature difference parameter on flow characteristics is illustrated graphically. It is observed that substantial influence has been exerted on flow characteristics, heat transfer rate (Nusselt number) and mass transfer rate (Sherwood number) for various values of transpiration parameter. The wall thermophoretic velocity changes according to the variation of physical parameters.

Keywords Thermophoresis · Thermal radiation · Non-Darcy · Suction/injection · Rotating cone

List of Symbols

C	Non-dimensional concentration
C_b	Forchheimer's inertial drag coefficient
C_L	Concentration at the cone base
c_p	Specific heat at pressure constant
D	Diffusivity of the molecule
$(Da)^{-1}$	Inverse Darcy number $\left(\frac{\nu}{k\Omega \sin \alpha}\right)$
g	Acceleration due to gravity
g_s	Mixed convection parameter $\left(\frac{Gr}{Re^2}\right)$
Gr	Grashof number $\left(\frac{g\beta_T(T_w - T_\infty)L^3 \cos \alpha}{\nu^2}\right)$
h_0	Dimensionless wall mass transfer Coefficient $\left(\frac{w_0}{(\nu\Omega \sin \alpha)^{\frac{1}{2}}}\right)$
K	Porous medium's permeability
k	Thermophoretic coefficient
k^*	Coefficient of mean absorption
k_e	Effective thermal conductivity
L	Cone slant height
Nt	Relative temperature difference parameter $\left(\frac{T_w - T_\infty}{T_\infty}\right)$
q_r	Heat flux of the thermal radiation
R	Thermal radiation parameter $\left(\frac{4\sigma^*(T_w - T_\infty)^3}{k^*k_e}\right)$
Re	Local Reynolds number $\left(\frac{\Omega L^2 \sin \alpha}{\nu}\right)$
T	Temperature (non-dimensional)
T_L	Temperature at cone surface
V_t	Thermophoretic velocity $\left(\frac{-k Pr}{Nt + \theta} \frac{\partial \theta}{\partial y}\right)$
w_0	Fluid suction at the cone surface

✉ B. Mallikarjuna
drbmallikarjuna.maths@gmail.com;
mallikarjuna.jntua@gmail.com

¹ Department of Mathematics, BMS College of Engineering, Bangalore 560019, India

² Department of Mathematics, Faculty of Science, Aswan University, 81528 Aswân, Egypt

³ College of Engineering -Mechanical Engineering Department, Babylon University, Babylon City, Hilla, Iraq

⁴ Department of Mathematics, Sri Veankateswara University, Tirupati, 517502 Andhrapradesh, India



Greek symbols

Γ	Forchheimer parameter (local inertia drag coefficient) $\left(\frac{C_b L}{\rho}\right)$
Ω	Rotational angular velocity
ρ	Density of the fluid
σ^*	Stefan–Boltzmann constant

1 Introduction

Mixed convective flow from a rotating cone is a branch of research undergoing fast growth in heat and mass transfer. This is quite common because of its enormous applications in geothermal, geophysical, environmental and energy and solutal-related engineering problems. Prominent applications are design of canisters for nuclear waste disposal, design of turbines, turbomachines, rotating heat exchangers, nuclear reactor cooling systems, spin stabilized missiles, geothermal reservoirs, estimating flight rotating wheel's path and in many geophysical vortices problems. Heat transfer process by free and forced convection from a rotating vertical cone embedded in a porous medium had been analyzed first by Hering and Grosh [1] and Himasekhar and Sarma [2]. The effect the generation of heat on convective boundary layer flow from rotating bodies (disks, cones and axisymmetric surfaces) has been investigated by Wang [3]. MHD and unsteady effects on convective flow past a rotating cone in porous medium have been presented by Chamkha [4] and Takhar [5]. Recently, Nadeem and Saleem [6] found approximate analytical solutions of unsteady combined free and forced convective flow of Newtonian fluid on a rotational cone with the influence of magnetic field. Mallikarjuna et al. [7] presented numerical results and investigated Darcy and chemical reaction effect on free and forced convective flow from a vertical rotating cone with variable porosity regime.

On the other side, the thermophoresis is the transport phenomenon of concentration molecule which leads to small particles are to be driven away from a heated surface and toward a cold one. It is a mass transfer mechanism to point out the particles on cold surfaces, particularly a significant for submicron dust particles since the velocity of thermophoretic is an independent of the size of the particle. In fact, submicrometer-sized dust particles are suspended in a non-isothermal gas with a gradient of temperature and influence a force in the direction contrary to the gradient of temperature. However, thermophoresis phenomenon was first introduced by Tyn-dall [8] when he presented a free dust layer in a dusty gas surrounding of a heat geometry. Recently, Shehzad et al. [9] studied thermophoresis influence on convective radiative flow of a Jeffery fluid with the influence of Joule heating. Kameswaran et al. [10] analyzed the influence of thermophoretic and nonlinear convection flow over a vertical

plate in a non-Darcy porous medium. Hariprasad et al. [11] investigated thermophoretic effect on heat and mass transfer flow of a mixed convection fluid over a vertical rotating cone with chemical reaction. Rashad et al. [12] and Mallikarjuna et al. [13] investigated thermophoresis effect on double diffusive convective flow induced by vertical rotating cone in a porous medium.

The suction/injection effects on double diffusive convective problems has great importance in extending theory of industrial- and engineering-related applications. The most prominent important application of suction (blowing) is in so-called transpiration cooling. If the suction fluid velocity is dissimilar from the free stream fluid flow an enhancement takes place in binary boundary layer regime. As well as energy and flow of fluid exchanges there is an exchange in molecules due to change in diffusion. Very light gases, for instance, hydrogen and helium have a great cooling effect. It can leads to clogging cooling process. Electronic devices are cooled by natural or mixed convection by giving sufficient number of outlets to enable heated air to leave and cooled air to enter. In fact, air blown is taking into account in case of inadequate of free convection cooling. All types of contaminants deliver in the air, such as moisture, lint and oil are situated on the body, causing overheating in this process. Hence, rate of flow volume of the air is to be controlled into the body, to reduce the deposition of the contaminants over the surface. This can be obtained accurately by evaluating heat and mass transfer near the boundary with thermophoresis effect. The Darcy convective flow over vertical rotating cone, suction/ injection effect is investigated by Himasekhar and Sarma [2] and Chamkha [4]. Recently, suction/ injection effect on heat transfer flow over shrinking sheet with radiation effect has been investigated by Bhattacharya [14]. Hamad and Ferdows [15] presented similarity solutions of convective orthogonal stagnation point flow from a stretching sheet in saturated nanofluid with suction/injection. Gangadhar and Bhaskar Reddy [16] studied chemical reaction and transpiration effects on double diffusive flow over a moving vertical plate. Rashidi et al. [17] found approximation analytical solutions to analyze transpiration effect on convective heat and mass transfer flow from a non-linearly stretching sheet in a fluid saturated nanofluid.

In view of the aforesaid applications, authors envisage to investigate transpiration and thermophoresis effect on double diffusive combined free and forced double diffusive convective flow from a vertical rotating cone in a non-Darcy porous medium. The numerical method is used to obtain the solutions of the differential equations pertinent to present physical model. The obtained results are compared with results available in the literature and very good agreement has been found. The results are presented graphically for the variation of thermophoresis parameter, transpiration parameter, inverse Darcy parameter and non-Darcy (Forchheimer) pa-



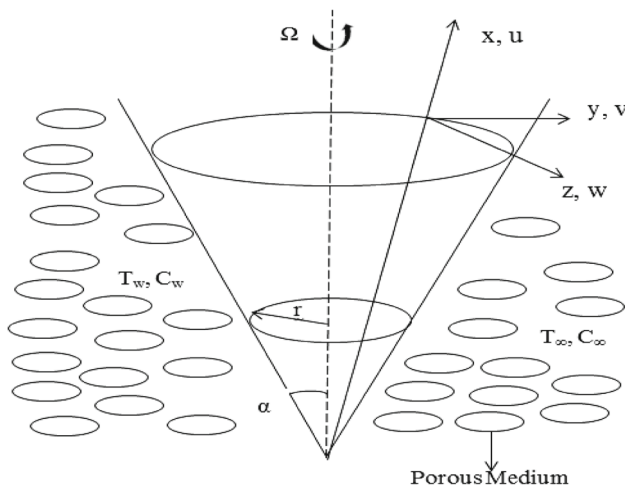


Fig. 1 Geometry of the model

parameter on fluid characteristics over the boundary layer and at surface of the cone.

2 Problem Formulation

Consider 2D steady viscous laminar incompressible flow from a permeable rotational vertical cone. Physical configuration is represented in Fig. 1. Here system of curvilinear coordinate is considered to describe the flow geometry. The x , y and z axes are along meridional section, circumferential section and normal to the cone, respectively. The cone is assumed with $T_w(x)$ and $C_w(x)$, free stream is assumed with constant temperature and concentration. The gray, absorbing and emitting fluid medium is assumed which is not scattered. Except the density, all the properties of porous medium and fluid are assumed to be constant. In the momentum equation, the density is assumed to be varying only in buoyancy force term. The porous region is to be described with non-Darcian Forchheimer drag force model. It contains first-order linear drag force for low influence velocity and second-order (quadratic) resistance, non-Darcy Forchheimer drag for high-velocity profiles. The non-Darcian Forchheimer model is therefore:

$$\nabla p = -\frac{\mu}{K}\mathbf{q} - \frac{\rho b}{K}\mathbf{q}^2$$

where \mathbf{q} is the general velocity, μ is the fluid dynamic viscosity, K is the porous medium permeability, across the porous medium p is the pressure drop and b is the inertial Forchheimer drag force. Using the boundary and Boussinesq approximation by taking into account of the above assumptions, the governing equations are:

$$\frac{u}{x} + \frac{\partial u}{\partial x} + \frac{\partial w}{\partial z} = 0 \quad (1)$$

$$\begin{aligned} u \frac{\partial u}{\partial x} + w \frac{\partial u}{\partial z} - \frac{v^2}{x} \\ = v \frac{\partial^2 u}{\partial z^2} - \frac{v}{K}u - \frac{C_b}{\rho}u^2 \\ + g\beta_t \left((T - T_\infty) + \frac{\beta_c}{\beta_t} (C - C_\infty) \right) \cos(\alpha) \end{aligned} \quad (2)$$

$$u \frac{\partial v}{\partial x} + w \frac{\partial v}{\partial z} + \frac{uv}{x} = v \frac{\partial^2 v}{\partial z^2} - \frac{v}{K}v - \frac{C_b}{\rho}v^2 \quad (3)$$

$$\left(u \frac{\partial T}{\partial x} + w \frac{\partial T}{\partial z} \right) = \frac{k_e}{\rho c_p} \frac{\partial^2 T}{\partial z^2} - \frac{1}{\rho c_p} \frac{\partial q_r}{\partial z} \quad (4)$$

$$u \frac{\partial C}{\partial x} + w \frac{\partial C}{\partial z} + \frac{\partial}{\partial z} (C v_t) = D \frac{\partial^2 C}{\partial z^2} \quad (5)$$

The appropriate boundary conditions are

$$\begin{aligned} \text{at } z = 0, \quad & \begin{cases} u(z) = 0, \quad v(z) = 0, \quad w(z) = -w_0 \\ T(z) = T_w(x), \quad C(z) = C_w(x) \end{cases} \\ \text{as } z \rightarrow \infty, \quad & \begin{cases} u \rightarrow 0, \quad v \rightarrow 0, \\ T \rightarrow T_\infty, \quad C \rightarrow C_\infty \end{cases} \end{aligned} \quad (6)$$

where (u, v, w) is the velocity vector along (x, y, z) , respectively.

$$\text{and } q_r = -\frac{4\sigma^*}{3k^*} \nabla T^4 \quad (7)$$

As less difference in the temperature of the fluid phase, T^4 can be arranged as a function of the temperature of degree 1. Using Taylor series about T_∞ and terminating terms of higher order, we get

$$\frac{\partial q_r}{\partial z} = \frac{16\sigma^* T_\infty^3}{3k^*} \frac{\partial^2 T}{\partial z^2} \quad (8)$$

Introducing the dimensionless transformations in Eqs. (1)–(6)

$$\begin{aligned} (u, v, w) &= (x\Omega \sin(\alpha) F(\eta), \\ &\quad x\Omega \sin(\alpha) G(\eta), (\nu\Omega \sin(\alpha))^{1/2} H(\eta)), \\ (T_w(x), C_w(x)) &= \left(T_\infty + \frac{(T_L - T_\infty)x}{L}, \right. \\ &\quad \left. C_\infty + \frac{(C_L - C_\infty)x}{L} \right), \\ \eta &= \frac{(\Omega \sin(\alpha))^{1/2}}{(\nu)^{1/2}} z, \quad \theta(\eta) = \frac{T - T_\infty}{T_w - T_\infty}, \\ r &= x \sin(\alpha), \quad \phi(\eta) = \frac{C - C_\infty}{C_w - C_\infty} \end{aligned} \quad (9)$$



Table 1 Results of $-H''(0)$ (skin friction coefficient in x -direction), $-G'(0)$ (skin friction coefficient in z -direction) and Nusselt number ($-\theta'(0)$) for mixed convection parameter (g_s) for $N = 0$, $R = 0$, $k = 0$, $\text{Pr} = 0.7$, $\Gamma = 0$, $h_0 = 0$ and $(\text{Da})^{-1} = 0$

$g_s = \text{Gr}/\text{Re}^2$	$-H''(0)$		$-G'(0)$		$-\theta'(0)$	
	Present values	Earlier values (Hering and Grosh [1])	Present values	Earlier values (Hering and Grosh [1])	Present values	Earlier values (Hering and Grosh [1])
0.1	1.13680	1.13690	0.65481	0.65489	0.46150	0.46156
10	8.5240	8.5246	1.4032	1.4037	1.0174	1.0173

Table 2 Nusselt number ($-\theta'(0)$) and skin friction coefficient in z -direction ($-G'(0)$) values for various values of h_0 for $N = 0$, $R = 0$, $k = 0$, $\text{Pr} = 0.7$, $\Gamma = 0$, $g_s = 1$ and $(\text{Da})^{-1} = 0$

Parameter	Earlier values (Himasekhar [2])	Present results	Earlier values (Himasekhar [2])	Present results
h_0	$-\theta'(0)$	$-\theta'(0)$	$-G'(0)$	$-G'(0)$
0.0	0.6114	0.6110	0.8427	0.8425
0.125	0.6416	0.6416	0.8810	0.8810
0.25	0.6724	0.6719	0.9194	0.9195
0.5	0.7354	0.7354	0.9968	0.9968
1.0	0.8668	0.8672	1.1534	1.1529

we get,

$$F = -\frac{1}{2}H' \quad (10)$$

$$H''' - HH'' + \frac{1}{2}(1 + \Gamma)(H')^2 - \text{Da}^{-1}H' \quad (11)$$

$$-2G^2 - 2\theta - 2N\phi = 0 \quad (12)$$

$$G'' - \Gamma G^2 - HG' + H'G - (\text{Da})^{-1}G = 0 \quad (13)$$

$$\frac{1}{\text{Pr}} \left(1 + \frac{4}{3}R\right) \theta'' + \left(\frac{1}{2}H'\theta - H\theta'\right) = 0 \quad (14)$$

$$\frac{1}{\text{Sc}} \phi'' + \frac{1}{2}H'\phi - H\phi' + \frac{Ntk}{\theta Nt + 1} \times \left(\phi'\theta' + \phi\theta'' - \frac{Nt\phi\theta'^2}{\theta Nt + 1}\right) = 0 \quad (15)$$

The conditions are transformed into

$$\begin{aligned} H'(0) &= 0, \quad H(0) = -h_0, \quad H'(\infty) \rightarrow 0, \\ G(0) &= 1, \quad G(\infty) \rightarrow 0, \\ \theta(0) &= 1, \quad \theta(\infty) \rightarrow 0, \quad \phi(0) = 1, \quad \phi(\infty) \rightarrow 0 \end{aligned} \quad (16)$$

The skin friction coefficients, local rate of heat and rate of mass transfer are presented by

$$\begin{aligned} C_{fx} &= \frac{2\mu \left(\frac{\partial u}{\partial z}\right)_{z=0}}{\rho (\Omega_0 x \sin \alpha)^2}, \quad C_{fy} = \frac{-2\mu \left(\frac{\partial v}{\partial z}\right)_{z=0}}{\rho (\Omega_0 x \sin \alpha)^2}, \\ \text{Nu}_x &= \frac{-x \left(\frac{\partial T}{\partial z}\right)_{z=0}}{(T_w - T_\infty)}, \quad \text{Sh}_x = \frac{-x \left(\frac{\partial C}{\partial z}\right)_{z=0}}{(C_w - C_\infty)} \end{aligned}$$

In dimensionless form:

$$\text{Re}^{1/2} C_{fx} = -H''(0) \quad (17)$$

$$2^{-1} \text{Re}^{1/2} C_{fy} = -G'(0) \quad (18)$$

$$\frac{\text{Nu}_x}{\text{Re}^{1/2}} = -\theta'(0) \quad (19)$$

$$\frac{\text{Sh}_x}{\text{Re}^{1/2}} = -\phi'(0) \quad (20)$$

3 Solution Procedure

A set of Eqs. (10)–(15) with specified conditions (16) are solved by employing numerical technique, i.e., shooting technique Mallikarjuna et al. [7], Rashad [12] and Srinivasacharya et al. [18, 19]. To validate the code, the current results are correlated with previously available results in the literature. Equations (23)–(28) coincide with equations presented by Hering and Grosh [1] Himasekhar et al. [2] by excluding concentration equation with thermophoresis influence, thermal radiation parameter and inverse Darcy parameters. The very good agreement has been found with previously published results as shown in Tables 1 and 2.

4 Results and Discussion

The fluid characteristics, i.e., flow velocity (tangential, circumferential and normal), heat and mass transfer profiles are presented graphically in Fig. 2, 3, 4, 5, 6, 7, 8, 9, 10, 11, 12, 13, 14, 15, 16, 16, 17, 18, 19, 20 and 21. The influence of inverse Darcy parameter $(\text{Da})^{-1}$, Forchheimer param-

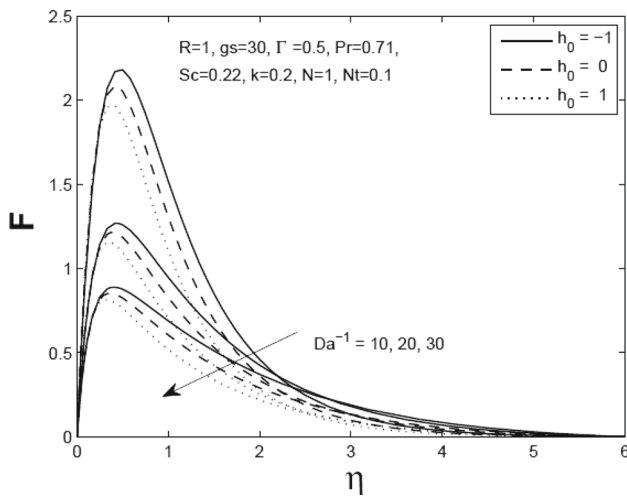


Fig. 2 Graph of F for various values of $(Da)^{-1}$ and h_0

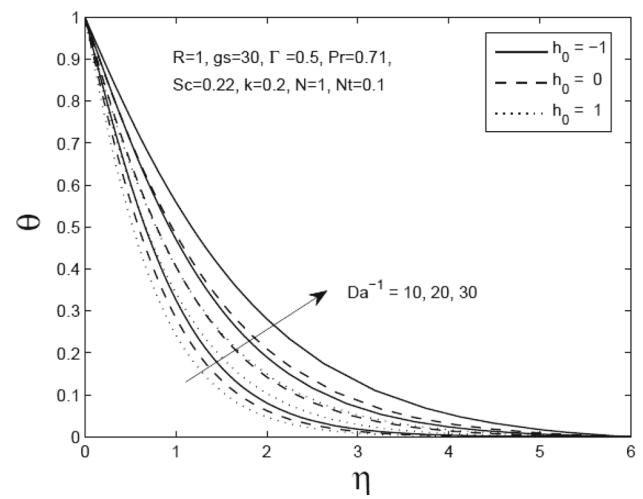


Fig. 5 Graph of θ for various values of $(Da)^{-1}$ and h_0

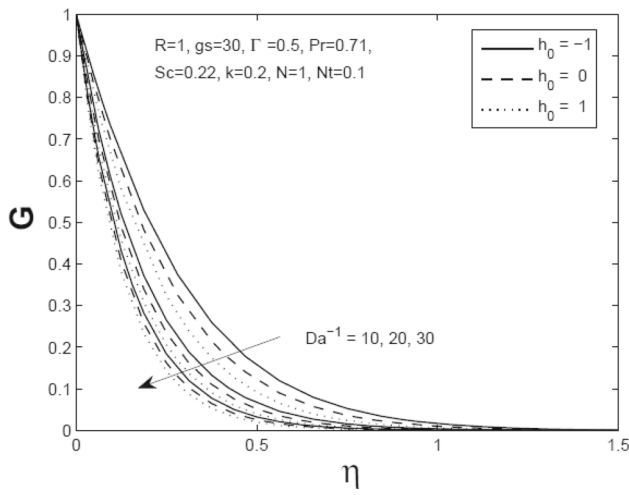


Fig. 3 Graph of G for various values of $(Da)^{-1}$ and h_0

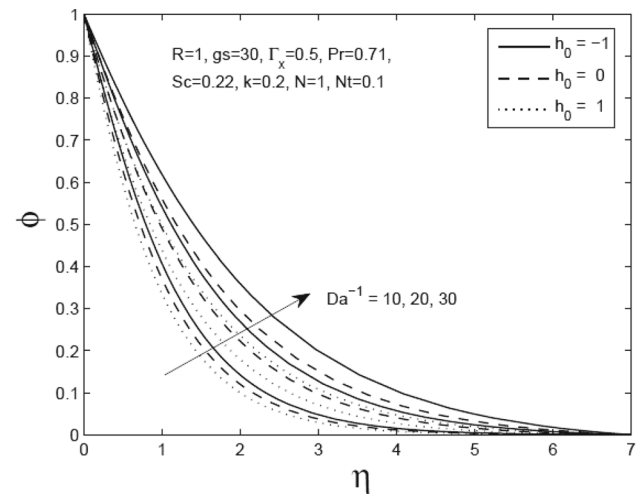


Fig. 6 Graph of ϕ for various values of $(Da)^{-1}$ and h_0

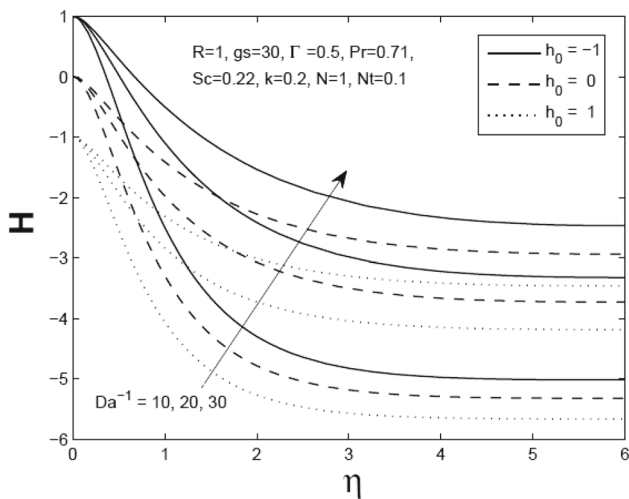


Fig. 4 Graph of H for various values of $(Da)^{-1}$ and h_0

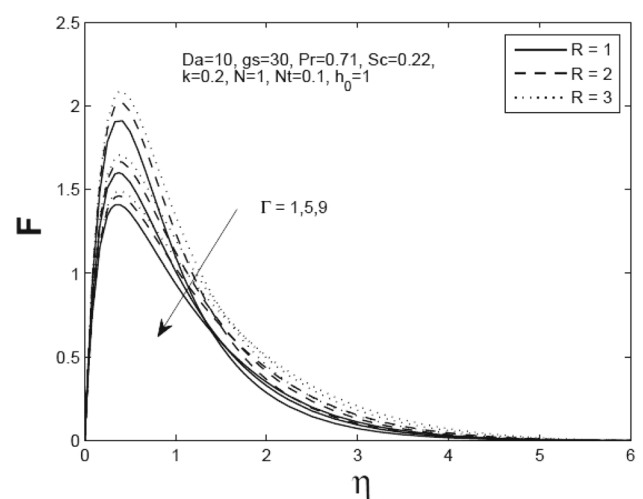


Fig. 7 Graph of F for various values of Γ and R

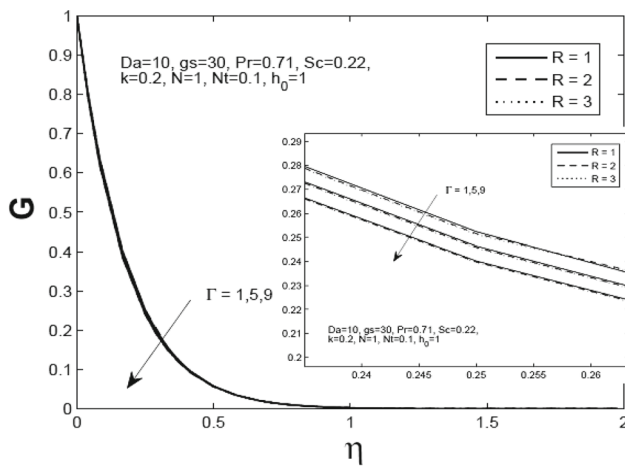


Fig. 8 Graph of G for various values of Γ and R

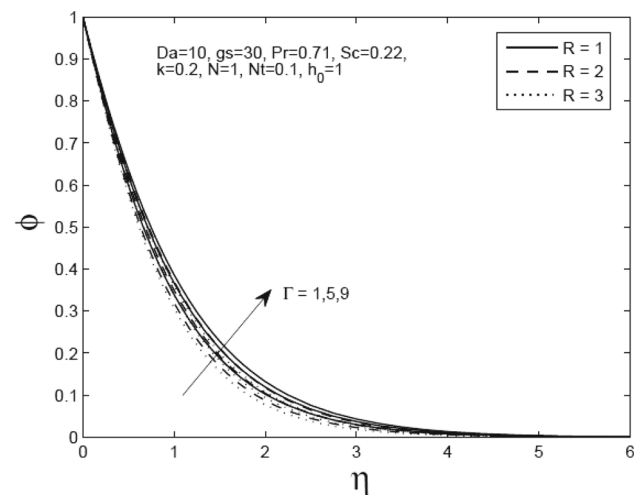


Fig. 11 Graph of ϕ for various values of Γ and R

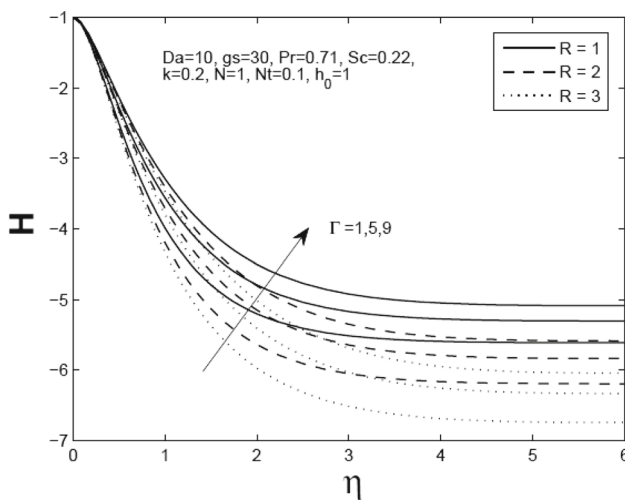


Fig. 9 Graph of H for various values of Γ and R

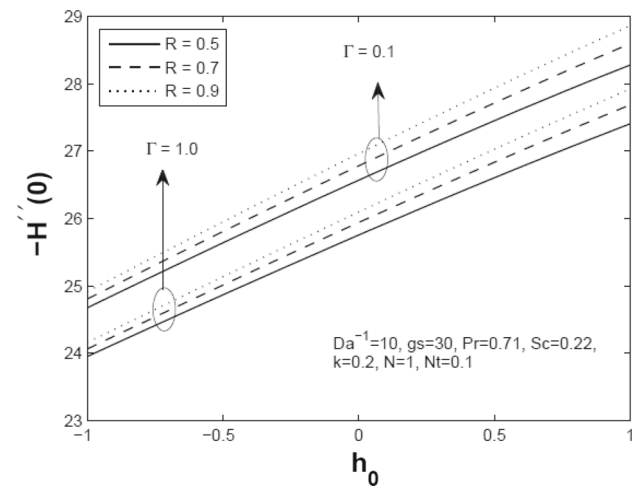


Fig. 12 Graph of $-H''(0)$ for various values of Γ and R

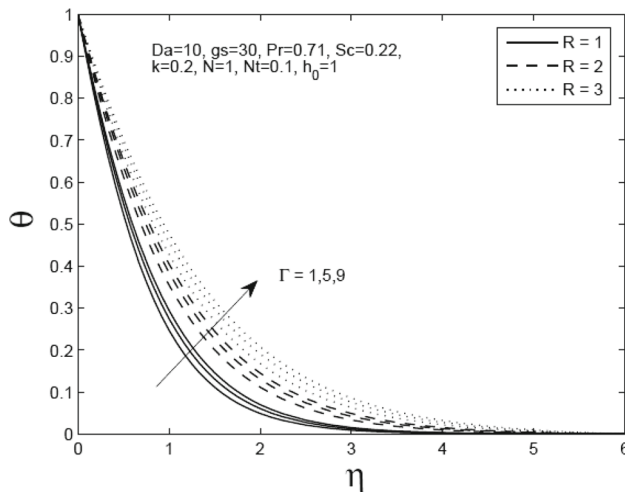


Fig. 10 Graph of θ for various values of Γ and R

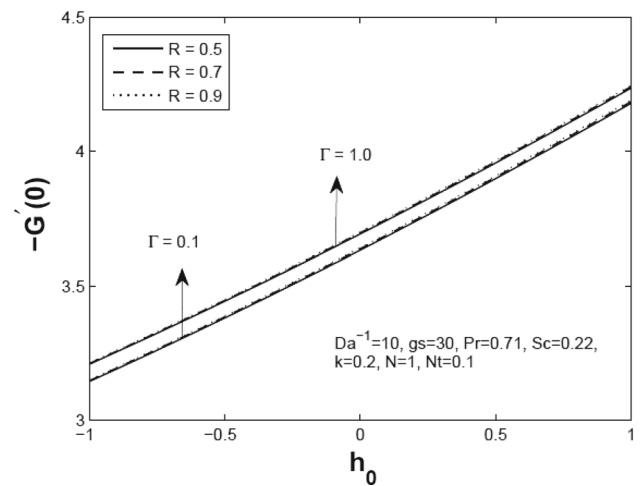


Fig. 13 Graph of $-G'(0)$ for various values of Γ and R

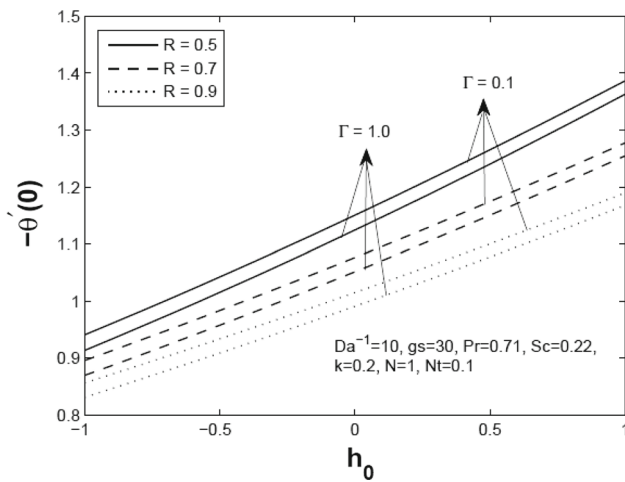


Fig. 14 Graph of $-\theta'(0)$ for various values of Γ and R

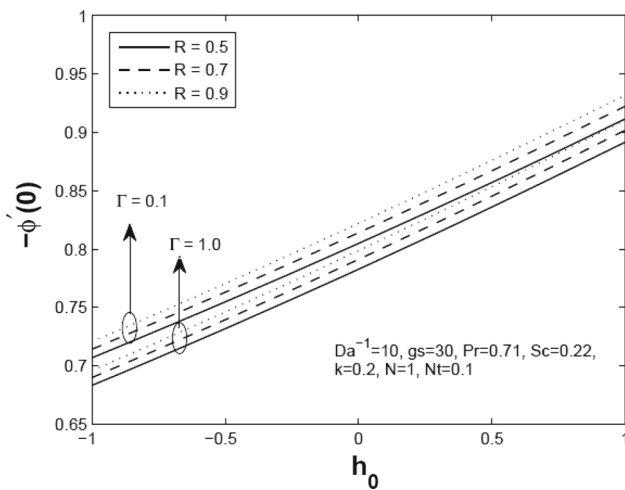


Fig. 15 Graph of $-\phi'(0)$ for various values of Γ and R

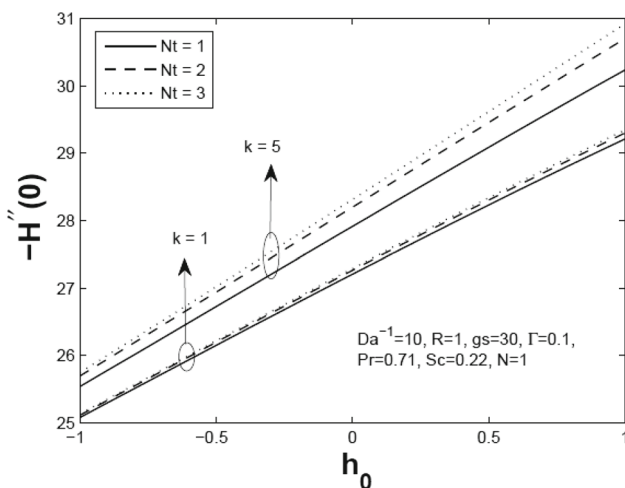


Fig. 16 Graph of $-H''(0)$ for various values of Nt and k

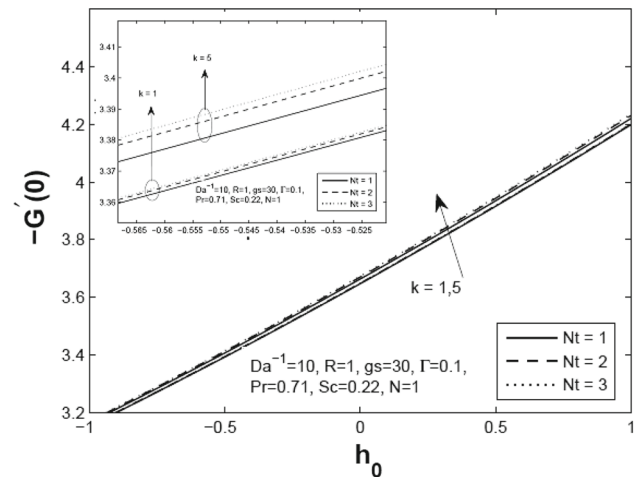


Fig. 17 Graph of $-G'(0)$ for various values of Nt and k

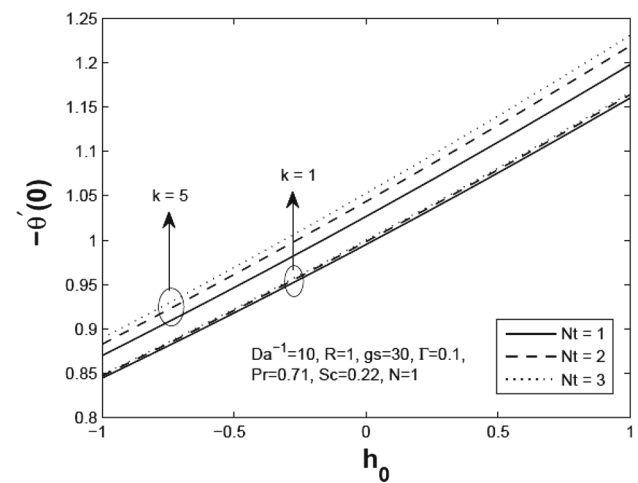


Fig. 18 Graph of $-\theta'(0)$ for various values of Nt and k

ter (Γ), suction/injection parameter (h_0), thermal radiation parameter R and thermophoretic coefficients (k) has been discussed. To analyze the influence of Da^{-1} , Γ , h_0 , R and k on the physical characteristics of the flow, the computations are carried out by fixing the other parameter values as $Pr = 0.71$, $gs = 30$, $Sc = 0.22$, $k = 0.2$, $Nt = 0.1$.

The effects of inverse Darcy parameter $(Da)^{-1}$ and suction $h_0 > 0$ and injection $h_0 < 0$ parameters on dimensional velocities (tangential, circumferential and azimuthal), temperature and concentration distributions are shown in Figs. 2, 3, 4, 5 and 6, respectively. As $(Da)^{-1} = \frac{\nu}{K\Omega \sin(\alpha)}$ increases, the porous medium permeability (K) decreases or viscosity is increases. It causes to reduce tangential and circumferential velocity fields with in the boundary layer regime as given in Figs. 2 and 3. A very strong enhancement in normal velocity profile, temperature and concentration distributions has been noticed from Figs. 4, 5 and 6, for larger values of Da^{-1} . A similar effect of inverse Darcy parameter on velocity and thermal diffusion fields has also been discussed by Chamkha



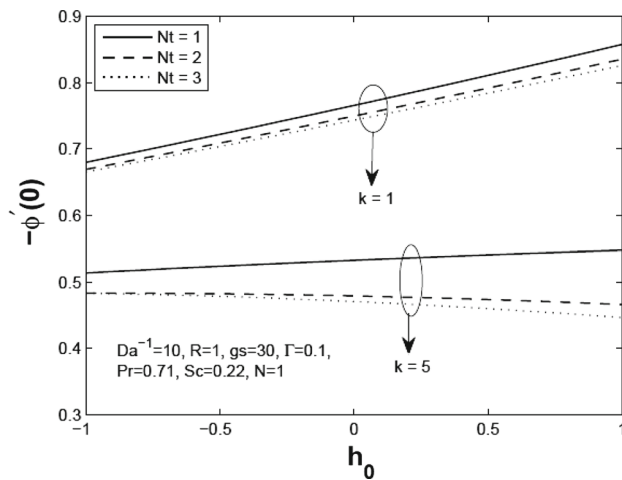


Fig. 19 Graph of $-\phi'(0)$ for various values of Nt and k

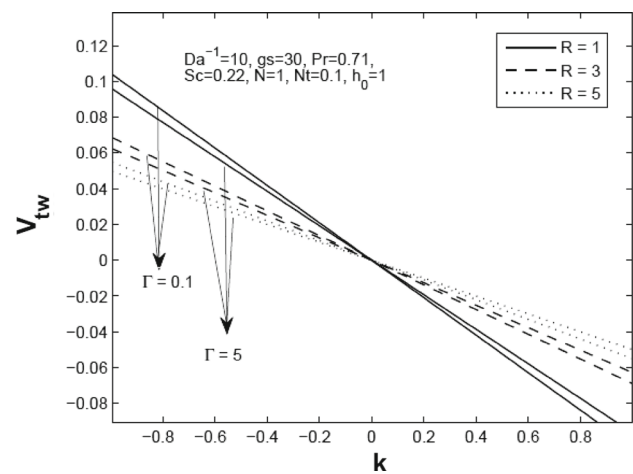


Fig. 21 Graph of V_{tw} for various values of R and Γ

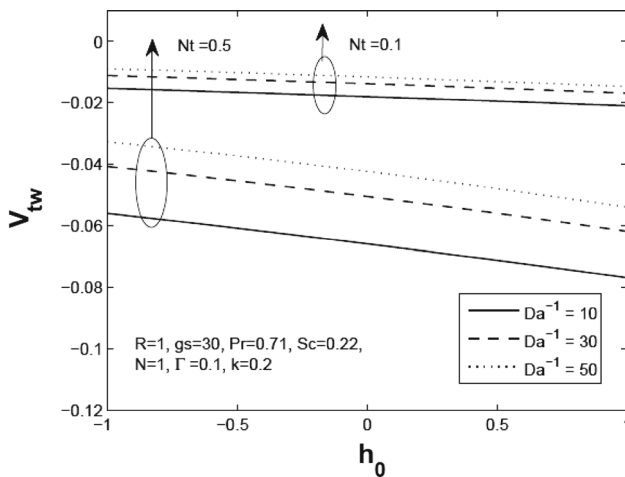


Fig. 20 Graph of V_{tw} for various values of Nt and $(Da)^{-1}$

[4]. The thickness of the thermal and concentration boundary layer increased for larger values of inverse Darcy parameter $(Da)^{-1}$. The transpiration velocity $h_0 = \frac{w_0}{(v\Omega \sin \alpha)^{1/2}}$ represents suction and injection corresponds to $h_0 > 0$ and $h_0 < 0$ and $h_0 = 0$ corresponds to an impermeable cone surface. We also observed from Figs. 2, 3, 4, 5 and 6 that the results are more dominated for the case of $h_0 < 0$. The similar behavior has been reported in Anwar Beg et al. [21] for spinning disk.

Figures 7, 8, 9, 10 and 11 illustrate the response to the parameters Forchheimer and thermal radiation parameters on non-dimensional velocity profiles, temperature and concentration distributions. The Forchheimer parameter $\Gamma = \frac{C_b L}{\rho}$ in the momentum Eqs. (11) and (13) is associated with Forchheimer second-order resistance term. Forchheimer inertial drag coefficient C_b is directly proportional to Forchheimer parameter Γ and has stronger influence adjacent to cone surface. Therefore, increase in Γ strongly retards tangential and circumferential velocities as presented in Figs. 7 and 8 while

enhancement in normal velocity profile (Fig. 9). The deceleration in the fluid flow serves to reduce in the thickness of the hydrodynamic boundary layer thickness which gives rise in energy and concentration diffusion and a thickening the boundary layer of thermal and concentration. Increasing radiation parameter R accelerates strongly, i.e., increases the fluid tangential velocity while reduce circumferential and normal velocity profiles. The radiation parameter $R = \frac{4\sigma^* T_\infty^3}{k^* k_e}$ in energy equation (14) states that “ratio of thermal radiation contribution relative to the thermal conduction.” For $R(<1) \rightarrow 0$ the term $\frac{4R}{3}$ tends to zero, thermal conduction contributes more than thermal radiation flux. For $R(>1) \rightarrow \infty$ i.e., R approaches to ∞ , thermal radiation dominates over thermal conduction. For $R = 1$, both thermal radiation and thermal conduction have the same contribution. We considered the last two of these three cases for present problem. Increasing thermal radiation contribution with an increase in R results strengthens the thermal diffusivity of the fluid and accelerated the thermal energy with in the thermal boundary layer. Therefore, temperature profile is increased with increase in R , as shown in Fig. 10. The boundary layer thickness for both velocity and thermal are increased with increasing contribution from thermal radiation (with decreasing contribution from thermal conduction). Conversely, there is considerable decrement in the concentration distribution for larger values of R , as observed in Fig. 11.

Figures 12, 13, 14 and 15 display the effect of thermal radiation (R), Forchheimer (Γ) and transpiration (h_0) parameters on skin friction coefficients in tangential ($C_{fx} Re_x^{1/2} = -H''(0)$) and azimuthal ($2^{-1} C_{fy} Re_x^{1/2} = -G'(0)$) (circumferential) directions, local rate of heat transfer ($Nu Re_x^{-1/2} = -\theta'(0)$) and mass transfer ($Sh Re_x^{-1/2} = -\phi'(0)$), respectively. The tangential and circumferential skin friction coefficients are found to be increasing for larger values of

R , i.e., with increasing thermal radiative flux (weaker thermal conduction effect) as given in Figs 12 and 13. Conversely, Nusselt number is observed to be reluctant with increasing R values, as presented in Fig. 14. Therefore, larger value of thermal radiation accelerates the fluid flow but reduces transport of thermal energy to the cone surface. Figure 15 shows that Sherwood number is to be strongly increased with increase in R . The greater contribution of thermal radiation heat transfer (and lower thermal conduction contribution) assists species diffusion to the cone surface. Overall the effect of thermal radiation in a porous media is clearly observed. Increasing Forchheimer parameter (Γ) retards the coefficient of skin friction along x -direction as well as enhance coefficient of skin friction in circumferential direction. Shear stress is considerably reduced, i.e., decelerate the friction coefficient along the surface of the cone, it causes to inhibit energy and species transport along the cone surface. The rate of heat transfer and mass transfer are therefore decreased with large values of Γ . An increase in h_0 (suction parameter) also accentuates the coefficients of the skin friction in x (tangential) and z (circumferential) directions, Nusselt and Sherwood numbers along the cone surface. Injection parameter ($h_0 < 0$) produced opposite results.

Figures 16, 17, 18 and 19 depict the influence of coefficient of thermophoretic (k) and relative temperature difference parameter (Nt) on coefficients of skin frictions, rate of heat transfer and mass transfer, respectively. Increase in thermophoretic coefficient (k) enhances coefficients of skin frictions, i.e., shear stress is strongly enhanced, caused to inhibit heat transfer rate along the cone surface. Nusselt number therefore increased with rise in thermophoretic coefficient. Conversely, Sherwood number reduced for increasing values of k . It is noticed from these figures that Nt reported similar results of the effect of k , i.e., skin friction coefficients and rate of heat transfer increases with increase in Nt from 1 to 3 but Sherwood number reduced.

Figures 20 and 21 represents the variation of thermophoretic velocity V_{tw} at cone surface for various values of inverse Darcy parameter, transpiration parameter, temperature difference parameter (Nt), thermophoretic coefficient (k), Forchheimer parameter and thermal radiation parameter. From Fig. 20, it is noticed that the wall thermophoretic velocity increased for larger values of Da^{-1} and injection parameter ($h_0 < 0$). The opposite results are reported for larger values of Nt and suction parameter ($h_0 > 0$). Figure 21 shows that increase in thermal radiation parameter is found to be an enhancement in wall thermophoretic velocity. The similar results reported for larger values of Forchheimer parameter. Conversely, wall thermophoretic velocity decelerates with a rise in k .

5 Conclusions

The effect of radiation, thermophoresis and transpiration parameters on free and forced combined convective flow over a rotating vertical cone in a saturated non-Darcy Forchheimer porous medium has been investigated. The governing boundary layer equations with conditions are converted into ODE by using specified transformations. Shooting technique is used to find the results of resultant equations. The influences of different physical parameters, thermophoretic coefficient, thermal radiation and transpiration, on fluid characteristics, were discussed for both the cases of Darcy and non-Darcy. An increase in thermal radiation causes to increase in tangential velocity profile and temperature distributions while depreciation in circumferential and normal velocity profile and concentration distribution. Drastic change in flow velocity, energy and molecular distribution has been reported for larger values of Forchheimer parameter compared to the inverse Darcy parameter. The coefficients of skin friction in x (tangential) and z (circumferential) directions and rate of heat transfer are found to enhance strongly with a rise in thermophoretic coefficient and relative temperature difference parameter while depreciation in Sherwood number. The thermophoretic velocity at the cone surface increases for larger values of thermal radiation, inverse Darcy parameter and Forchheimer parameters, and opposite trend has been noticed for larger values of thermophoretic coefficient, relative temperature difference parameter and transpiration parameter.

Acknowledgments The author Dr. Bandaru Mallikarjuna thanks to B.M.S College of Engineering (Autonomous), Bangalore-19, for providing financial assistance and kind support through the TEQIP [“Technical Education Quality Improvement Programme”] of the MHRD, Government of India.

References

1. Hering, R.G.; Grosh, R.J.: Laminar combined convection from a rotating cone. *ASME J. Heat Transf.* **85**, 29–34 (1963)
2. Himasekhar, K.; Sarma, P.K.: Effect of suction on heat transfer rates from a rotating cone. *Int. J. Heat Mass Transf.* **29**(1), 164–167 (1986)
3. Wang, C.Y.: Boundary layers on rotating cones, discs and axisymmetric surfaces with a concentrated heat source. *Acta Mech.* **81**, 245–251 (1990)
4. Chamkha, A.J.: Magnetohydrodynamic mixed convection from a rotating cone embedded in a porous medium with heat generation. *J. Porous Media* **2**(1), 87–106 (1999)
5. Takhar, H.S.; Chamkha, A.J.; Nath, G.: Unsteady mixed convection flow from a rotating vertical cone with a magnetic field. *Heat Mass Transf.* **39**, 297–304 (2003)
6. Nadeem, S.; Saleem, S.: Analytical treatment of unsteady mixed convection MHD flow on a rotating cone in a rotating frame. *J. Taiwan Inst. Chem. Eng.* **44**, 596–604 (2013)



7. Mallikarjuna, B.; Rashad, A.M.; Chamkha, A.J.; Hariprasad Raju, S.: Chemical reaction effects on MHD convective heat and mass transfer past a rotating vertical cone embedded in a variable porosity regime. *Afrika Matematika* **27**(3), 646–665 (2016)
8. Tyndall, J.: On dust and disease. *Proc. R. Inst. G.B.* **6**, 1–14 (1870)
9. Shehzad, S.A.; Alsaedi, A.; Hayat, T.: Influence of thermophoresis and Joule heating on the radiative flow of Jeffery fluid with mixed convection. *Braz. J. Chem. Eng.* **30**(4), 897–908 (2013)
10. Kameswaran, P.K.; Sibanda, P.; Partha, M.K.; Murthy, P.V.S.N.: Thermophoretic and nonlinear convection in non-Darcy porous medium. *ASME J. Heat Transf.* **136**, 042601–19 (2014)
11. Hariprasad Raju, S.; Mallikarjuna, B.; Varma, S.V.K.: Thermophoretic effect on double diffusive convective flow of a chemically reacting fluid over a rotating cone in porous medium. *Int. J. Sci. Eng. Res.* **6**(1), 198–204 (2015)
12. Rashad, A.M.; Mallikarjuna, B.; Chamkha, A.J.; Hariprasad Raju, S.: Thermophoresis effects on heat and mass transfer from a rotating cone in a porous medium with thermal radiation. *Afrika Matematika*, Article in press (2016). doi:[10.1007/s13370-016-0421-4](https://doi.org/10.1007/s13370-016-0421-4)
13. Mallikarjuna, B.; Rashidi, M.M.; Hariprasad Raju, S.: Influence of nonlinear convection and thermophoresis on heat and mass transfer from a rotating cone to fluid flow in porous medium. *Therm. Sci.*, Accepted and Article in Press. doi:[10.2298/TSCI150619004B](https://doi.org/10.2298/TSCI150619004B)
14. Bhattacharya, K.: Effects of radiation and heat source/sink on unsteady MHD boundary layer flow and heat transfer over a shrinking sheet with suction/ injection. *Front. Chem. Sci. Eng.* **5**(3), 376–384 (2011)
15. Hamad, M.A.A.; Ferdows, M.: Similarity solution of boundary layer stagnation point flow towards a heated porous stretching sheet saturated with a nanofluid with heat absorption/generation and suction/blowing: a lie group analysis. *Commun. Nonlinear Sci. Numer. Simul.* **17**, 132–140 (2012)
16. Gangadhar, K.; Bhaskar Reddy, N.: Chemically reacting MHD boundary layer flow of heat and mass transfer over a moving vertical plate in a porous medium with suction. *J. Appl. Fluid Mech.* **6**(1), 107–114 (2013)
17. Rashidi, M.M.; Freidoonimehr, N.; Hosseini, A.; Anwar Beg, O.; Hung, T.K.: Homotopy simulation of nanofluid dynamics from a non-linearly stretching isothermal permeable sheet with transpiration. *Meccanica* **49**, 469–482 (2014)
18. Srinivasacharya, D.; Mallikarjuna, B.; Bhuvanavijaya, R.: Soret and Dufour effects on mixed convection along a vertical wavy surface in a porous medium with variable properties. *Ain Shams Eng. J.* **6**, 553–564 (2015)
19. Srinivasacharya, D.; Mallikarjuna, B.; Bhuvanavijaya, R.: Natural convection along a vertical wavy surface in a porous medium with variable properties and cross diffusion effects. *Int. J. Nonlinear Sci.* **19**(1), 53–64 (2015)
20. Anwar Beg, O.; Zueco, J.; Lopez-Ochoa, L.M.: Network numerical analysis of optically thick hydromagnetic slip flow from a porous spinning disk with radiation flux, variable thermophysical properties, and surface injection effects. *Chem. Eng. Commun.* **198**, 360384 (2011)
21. Anwar Beg, O.; Zueco, J.; Ghosh, S.K.: Unsteady hydromagnetic natural convection of a short-memory viscoelastic fluid in a non-Darcian regime: network simulation. *Chem. Eng. Commun.* **198**, 172–90 (2010)

